

Neutron induced fission cross section measurements of ^{240}Pu and ^{242}Pu

F. Belloni^{1a}, R. Eykens¹, J. Heyse¹, C. Matei², A. Moens¹, R. Nolte³, A.J.M. Plompen¹, S. Richter¹, G. Sibbens¹, D. Vanleeuw¹, and R. Wynants¹

¹ European Commission, JRC-Geel, 2440 Geel, Belgium

² National Physical Laboratory, Teddington TW11 0LW, UK

³ Physikalisch-Technische Bundesanstalt, 38116 Braunschweig, Germany

Abstract. Accurate neutron induced fission cross section of ^{240}Pu and ^{242}Pu are required in view of making nuclear technology safer and more efficient to meet the upcoming needs for the future generation of nuclear power plants (GEN-IV). The probability for a neutron to induce such reactions figures in the NEA Nuclear Data High Priority Request List [1].

A measurement campaign to determine neutron induced fission cross sections of ^{240}Pu and ^{242}Pu at 2.51 MeV and 14.83 MeV has been carried out at the 3.7 MV Van De Graaff linear accelerator at Physikalisch-Technische Bundesanstalt (PTB) in Braunschweig. Two identical Frisch Grid fission chambers, housing back to back a ^{238}U and a ^{242}Pu target ($A = 240$ or $A = 242$), were employed to detect the total fission yield. The targets were molecular plated on 0.25 mm aluminium foils kept at ground potential and the employed gas was P10. The neutron fluence was measured with the proton recoil telescope (T1), which is the German primary standard for neutron fluence measurements. The two measurements were related using a De Pangher long counter and the charge as monitors. The experimental results have an average uncertainty of 3–4% at 2.51 MeV and for 6–8% at 14.81 MeV and have been compared to the data available in literature.

1. Introduction

Three out of the six nuclear energy systems chosen by the Generation IV International Forum are fast neutron reactors. Plutonium will represent up to 20% in weight of the first load fuel composition of Gas Cooled Fast Reactors [2], and will exceed 26% in the MYRRHA accelerator driven system demonstrator [3]. High accuracy neutron induced cross section data on the even-even isotopes of plutonium, among others, are therefore needed. An uncertainty reduction of up to 10% is required on ^{242}Pu $\sigma_{(n,f)}$ in the neutron kinetic energy region between 2.23 MeV and 6.07 MeV and of up to 24% between 6.07 MeV and 19.6 MeV. The accuracy on ^{240}Pu $\sigma_{(n,f)}$ needs to be improved from the present 5% to the demanded 3% in the neutron kinetic energy region between 2.23 MeV and 6.07 MeV [4].

2. Experimental set-up

The 3.7 MV Van De Graaff linear accelerator at the Physikalisch-Technische Bundesanstalt (PTB) in Braunschweig was used to produce monoenergetic neutron beams of 2.51 MeV and 14.83 MeV kinetic energy through $p+^3\text{H}$ and $d+^3\text{H}$ reactions respectively. Two identical Frisch Grid fission chambers were manufactured in JRC-Geel. One was loaded with 0.808 (16) mg of ^{238}U in a $\text{U}(\text{OH})_4$ target (assuming the layer is a hydroxide) back to back with a 0.0971 (4) mg of ^{240}Pu in a $\text{Pu}(\text{OH})_4$ deposit (always assuming the layer is a hydroxide, here as in the

rest of the text), and the other with 0.861 (16) mg of ^{238}U (in $\text{U}(\text{OH})_4$) back to back with a 0.625 (5) mg of ^{242}Pu (in $\text{Pu}(\text{OH})_4$). The target references are respectively TP2011-008-07, TP2011-011-06, TP-2011-008-03x and TP2010-012-03 [5]. All targets were molecular plated on 0.25 mm aluminium foils kept at ground potential. On the uranium side, the charges produced through ionization in P10 were collected by an anode positioned at 6 mm from the deposit. The gas volume on the plutonium side was instead larger. A grid was located at 3 cm from the target, followed by an anode at an additional distance of 6 mm. The ^{238}U , ^{240}Pu and ^{242}Pu distances to the neutron converter and the resulting beam energy spreads are summarized in Table 1.

3. Neutron flux measurement

The neutron fluence was measured with the proton recoil telescope (PRT) T1, which is the German primary standard for neutron fluence measurements between 1.2 MeV and 20 MeV and with a De Pangher long counter (PLC) [6]. During dedicated runs, the fission chambers were moved away from the beam at backward angles, the PRT was positioned at 0 degrees with respect to the ion beam line, at a distance from the neutron producing target varying between 20 cm and 35 cm, and the fluence was extracted from the T1 with reference to the (n,p) elastic cross sections (ENDF/B-V). In the same time, the counts detected by the PLC were registered. The neutron fluence during the neutron induced fission measurements was extracted from the De Pangher long counter [6] calibrated on the PRT as described above. The

^a e-mail: francesca.belloni@cea.fr

Table 1. Experimental conditions.

	Detector loaded with			
	^{238}U & ^{240}Pu		^{238}U & ^{242}Pu	
E_n (MeV)	2.51	14.83	2.51	14.83
Distance (mm)	158.6	206.6	158.6	206.7
target to converter	& 159.1	& 207.1	& 159.2	& 207.2
FWHM (MeV)	0.14	0.57	0.14	0.57

De Pangher long counter was positioned at 98° relative to the direction of the ion beam. Alternatively the fluence for the fission measurements could be determined using the charge collected on the neutron production target and the fluence/charge factor obtained with the PRT.

For comparison the neutron fluence was measured also using the Frisch Grid fission chambers and the standard neutron induced fission cross sections of ^{238}U [7].

4. Data analysis

The neutron induced fission cross sections were calculated from the number of nuclei n of the investigated isotopes in the target, the amount N of detected fission fragments (FFs), and the measured neutron fluence $\Phi(E)$:

$$\sigma_{n,f}(E) = \frac{N}{\Phi(E) \cdot n \cdot \epsilon(E) \cdot f(E)} \quad (1)$$

The detection efficiency $\epsilon(E)$ of the ionization chamber for fission fragments (FFs) generated by neutrons of kinetic energy E accounts both for the number of FFs producing a signal below threshold and the amount of FFs trapped inside the target. The factor $f(E) = c_{LT}/c(E)_{ms}$ includes the live time (LT) and the multiple scattering corrections.

The ionization chambers were operated in pulse mode. A threshold was imposed on the pulse height spectra (PHS) in order to discriminate FFs from α particles. The number N was obtained by integrating the spectra from threshold to full-scale in background (“beam off”) and foreground (“beam on”) measurements and by subtracting the first contribution from the second to discard the spontaneous fission (SF) events.

GEANT4 simulations were carried out to determine the fraction of FFs trapped inside the targets for background and “beam on” conditions. The multiple scattering corrections were calculated with the help of the MCNP code, by comparing the neutron induced fission reaction rate obtained in a target located at the desired position from the neutron source and surrounded by vacuum with the neutron induced fission reaction rate in the same deposit inserted in the fission chamber.

The live time of the electronic chains connected to each electrode was measured with a pulser and calculated by dividing the number of delivered pulses by the number of detected pulses. The same pulser was used to inject signals of decreasing voltage in all electronic chains and the corresponding PHS were recorded, allowing an offset determination.

The amount of FFs producing a signal below threshold was extracted following two different methodologies.

4.1. Fitting method

The low energy tail of the PHS in background and “beam on” conditions was fitted with an exponential superimposed to a flat background ($y = \exp^{p_0+p_1 \cdot x} + p_2$). The integral between the offset and the threshold pulse amplitudes of the fit performed on a region delimited by a minimum and maximum channel ($[\text{min_ch}, \text{max_ch}] \subseteq [\text{offset}, \text{threshold}]$) gives the number of FFs entering the gas, and producing a signal so low that it is discarded by the ADC threshold or is recorded in the α background region. The error bar associated to the number of FFs calculated this way is obtained as the deviation from such number when the lower or the upper limit of the fitting region is varied by one channel. The four fitting region configurations used to calculate the error bar associated to the number of FFs are: $[\text{min_ch}+1, \text{max_ch}]$, $[\text{min_ch}-1, \text{max_ch}]$, $[\text{min_ch}, \text{max_ch}+1]$, $[\text{min_ch}, \text{max_ch}-1]$.

This analysis method revealed to be quite subjective since changing by one single channel the fitting region, the calculated cross sections significantly change. For example, the value obtained for ^{240}Pu $\sigma_{n,f}$ increases by 1.8% when the fitting region is $[\text{min_ch}-1, \text{max_ch}]$, while it decreases by 4.3% if the fit is performed between $[\text{min_ch}+1, \text{max_ch}]$. In view of this sensitivity to the choice of threshold this method is not reliable and we had to resort to a second method.

4.2. Efficiency method

The procedure is based on the assumption that the PHS of the anode signals in background and beam conditions show no significant difference. This allows to introduce a detection efficiency “R”, defined as the ratio of the amount of SF events above threshold in background condition to the total number of expected SF events during a certain interval, calculated from the half life of the considered isotope. The value of R will be the same for a SF spectrum and a neutron induced fission spectrum, provided that the same isotope is considered. Given R and the integral of the neutron induced PHS above threshold, the number of FFs below threshold can be computed. The error bar associated to the counting statistics is calculated by error propagation of the quantities involved in its determination.

5. Results

The neutron induced fission cross sections of ^{240}Pu and ^{242}Pu measured at 2.51 MeV and 14.83 MeV are reported in Table 2.

Our final results are those of the Efficiency method. For completeness we also show the result of the Fitting procedure which are clearly biased. From the Table 2 it is evident that the data at 14.83 MeV have larger uncertainties. This is a combination of the counting statistics and the value of the ^{238}U $\sigma_{n,f}$, which is higher at higher neutron energies and is directly proportional to the flux. The neutron flux extracted from ^{238}U data is always in agreement with the one provided by PTB within its accuracy (2.9%).

The live times of the electronic chains are similar, and range between $99.83\% \pm 0.04\%$ and $99.93\% \pm 0.04\%$. The percentage of FFs trapped in the targets is higher for the thicker ^{242}Pu (average 2.29%) than for the thinner

Table 2. Measured neutron induced fission cross sections.

$\sigma_{(n,f)}^{240}\text{Pu} @ E_n = 2.51 \text{ MeV}$	
Fitting method (flux from PTB)	$(1.63 \pm 0.06) \text{ b}$
Fitting method (flux from ^{238}U)	$(1.61 \pm 0.06) \text{ b}$
Efficiency method (flux from PTB)	$(1.75 \pm 0.06) \text{ b}$
Efficiency method (flux from ^{238}U)	$(1.74 \pm 0.06) \text{ b}$
$\sigma_{(n,f)}^{240}\text{Pu} @ E_n = 14.83 \text{ MeV}$	
Fitting method (flux from PTB)	$(2.32 \pm 0.15) \text{ b}$
Fitting method (flux from ^{238}U)	$(2.28 \pm 0.15) \text{ b}$
Efficiency method (flux from PTB)	$(2.41 \pm 0.15) \text{ b}$
Efficiency method (flux from ^{238}U)	$(2.36 \pm 0.09) \text{ b}$
$\sigma_{(n,f)}^{242}\text{Pu} @ E_n = 2.51 \text{ MeV}$	
Fitting method (flux from PTB)	$(1.41 \pm 0.06) \text{ b}$
Fitting method (flux from ^{238}U)	$(1.41 \pm 0.06) \text{ b}$
Efficiency method (flux from PTB)	$(1.47 \pm 0.06) \text{ b}$
Efficiency method (flux from ^{238}U)	$(1.47 \pm 0.06) \text{ b}$
$\sigma_{(n,f)}^{242}\text{Pu} @ E_n = 14.83 \text{ MeV}$	
Fitting method (flux from PTB)	$(2.17 \pm 0.12) \text{ b}$
Fitting method (flux from ^{238}U)	$(2.22 \pm 0.14) \text{ b}$
Efficiency method (flux from PTB)	$(2.20 \pm 0.12) \text{ b}$
Efficiency method (flux from ^{238}U)	$(2.25 \pm 0.16) \text{ b}$

^{240}Pu (0.75%) and is considered error free. The multiple scattering corrections calculated with the MCNP code have an average statistical uncertainty of 0.23%.

The upper panel of Fig. 1 shows the comparison among the experimental ^{240}Pu neutron induced fission cross sections collected from 1960 to 2016 in the energy region between 2 MeV and 3 MeV. Only those data sets reporting directly cross sections in EXFOR were considered. The same holds for all graphs. The only two sets of measurements reporting a point at 2.5 MeV are the ones of Salvador-Castiñeira [10] and of Tovesson [8]. For all other measurements, linear interpolation between points is used to draw conclusions. Our data extracted with the “efficiency method” are in good agreement with Tovesson [8] and Kari [9]. Salvador-Castiñeira data [10] and Nesterov [12] agree, within the error bars, with our results while Laptev [11] and Meadows [13] report respectively much lower and slightly lower values which do not agree within the error bars with our data.

The comparison among the experimental ^{240}Pu neutron induced fission cross section data sets available in the energy region between 14.5 MeV and 15.5 MeV is reported in the lower panel of Fig. 1. No data were measured at 14.8 MeV, therefore again the linear interpolation between points is used to draw conclusions. All data agree with each other within the error bars. As in the lower energy region, our results are closer to Tovesson [8].

The comparison among the available ^{242}Pu neutron induced fission cross section between 2 MeV and 3 MeV is reported in the upper panel of Fig. 2. Tovesson data [8] this time are not in agreement with our results. This also applies to the data of Meadows [14]. Bergen [15], Salvador-Castiñeira [10], Auchampaugh [17] and Weigmann [16] agree with our data within the error bars.

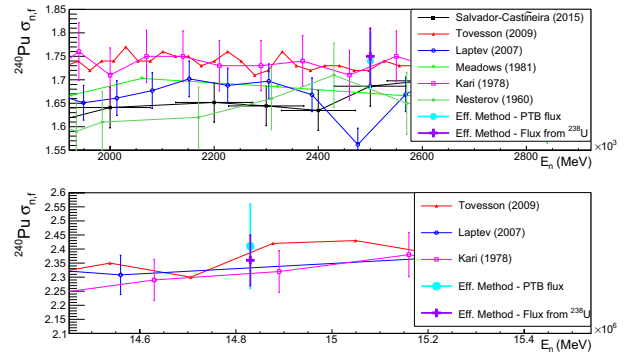


Figure 1. Experimental neutron induced fission cross sections of ^{240}Pu in the energy region between 2 MeV and 3 MeV (upper panel) and between 14.5 MeV and 15.5 MeV (lower panel).

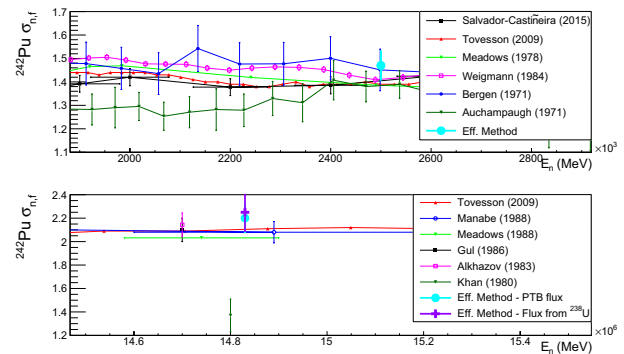


Figure 2. Experimental neutron induced fission cross sections of ^{242}Pu in the energy region between 2 MeV and 3 MeV (upper panel) and between 14.5 MeV and 15.5 MeV (lower panel).

The lower panel of Fig. 2 shows the comparison among the available ^{242}Pu $\sigma_{n,f}$ experimental cross sections in the neutron energy ranging from 14.5 MeV to 15.5 MeV.

Tovesson [8] and Manabe [18] agree with all our results. Not much can be said for Gul [19] and Alkhazov [20], since the energy is not exactly the same and only one data point is available for each of these measurements. Khan [21] and Meadows [22] result to be lower than all other data.

6. Conclusions

Neutron induced fission cross section measurements of ^{242}Pu and ^{240}Pu at 2.51 MeV and 14.83 MeV have been performed at the 3.7 MV Van De Graaff linear accelerator at Physikalisch-Technische Bundesanstalt (PTB) in Braunschweig. Two analysis methods have been employed and the results are mainly in agreement with the experimental data collected in the past. The results confirm that the ^{242}Pu $\sigma_{n,f}$ measured at 14.8 MeV by Khan [21] and Meadows [22] seem to be too low. To exclude other data, higher accuracy is needed.

This work was partly supported by the EMRP ENG08 METROFISSION project of the European Metrology Research Programme which is jointly funded by EURAMET and the European Union. The authors thank the operators of the PTB

VdG accelerator for providing the conditions necessary for these experiments.

References

- [1] OECD-NEA High priority request list for nuclear data (HPRL), www.oecd-nea.org/dbdata/hpr1
- [2] US DOE Nuclear Energy Research Advisory Committee, Generation IV International Forum, USA (2002) Report No.: GIF-002-00
- [3] V. Scanziani and M.L. Bonardi and F. Groppi and S. Manenti and P. Pierini, SIS Pubblicazioni Laboratori Nazionali di Frascati, 2010 Jul 05
- [4] M. Salvatores et al., Report NEA/WPEC-26, Paris 2008
- [5] Sibbens, G., Moens, A., Eykens, R. et al. J Radioanal Nucl Chem (2014) **299**, 1093, doi: 10.1007/s10967-013-2668-7
- [6] R. Nolte and D.J. Thomas, Metrologia **48**, 6, S274
- [7] A.D. Carlson et al., Nuclear Data Sheets **110**, 12, December 2009, p. 3215-3324
- [8] F. Tovesson, T.S. Hill, M. Mocko, J.D. Baker, C.A. Mcgrath, Physical Review C **79**, 014613 (2009)
- [9] K. Kari, S. Cierjacks, Report: Kernforschungszentrum Karlsruhe Reports No. 2673 (1978)
- [10] P. Salvador-Castifeira, T. Bryś, R. Eykens, F.-J. Hamsch, A. Göök, A. Moens, S. Oberstedt, G. Sibbens, D. Vanleeuw, M. Vidali, and C. Pretel, Phys. Rev. C **92**, 014620 (2015)
- [11] A.B. Laptev, A.Yu. Donets, V.N. Dushin, A.V. Fomichev, A.A. Fomichev, R.C. Haight, O.A. Shcherbakov, S.M. Soloviev, Yu.V. Tuboltsev, A.S. Vorobiev, R.C. Haight, A.D. Carlson, Nuclear Physics, Section A **734**(1), E45 (2007)
- [12] V.G. Nesterov, G.N. Smirenkin, Atomnaya Energiya **9**(1), 16 (1960)
- [13] J.W. Meadows, Nuclear Science and Engineering **79**, 233 (1981)
- [14] J.W. Meadows, Nuclear Science and Engineering **68**, 360 (1978)
- [15] D.W. Bergen, R.R. Fullwood, Nuclear Physics A **163**, 577 (1971)
- [16] H. Weigmann, J.A. Wartena, C. Burkholz, EXFOR Data 21931002. Nucl. Phys. A **438**, 333 (1985)
- [17] G.F. Auchampaugh, J.A. Farrell, D.W. Bergen, Nuclear Physics A **171**, 31 (1971)
- [18] F. Manabe, K. Kanda, T. Iwasaki, H. Terayama, Y. Karino, M. Baba, N. Hirakawa, Fac. of Engineering, Tohoku Univ. Tech. Report **52**(2), 97 (1988)
- [19] K. Gul, M. Ahmad, M. Anwar, S.M. Saleem, Nuclear Science and Engineering **94**, 42 (1986)
- [20] I.D. Alkhazov, E.A. Ganza, L.V. Drapchinskij, V.N. Dushin, S.S. Kovalenko, O.I. Kostochkin, K.A. Petrzhak, A.V. Fomichev, V.I. Shpakov, R. Arlt, W. Wagner, M. Josch, G. Musiol, H.-G. Ortlepp, G. Pausch, Conf 3. Meet. on Neutron Radiation Metrology, Moscow (1983) **2**, p. 201
- [21] N.A. Khan, H.A. Khan, K. Gul, R.A. Akber, M. Anwar, A. Waheed, G. Hussain, M.S. Shaikh, Nuclear Instrum. and Methods in Physics Res. **173**, 13 (1980)
- [22] J.W. Meadows, Annals of Nuclear Energy **15**, 421 (1988)